ELSEVIER

Catalysis Today 46 (1998) 13–26

CATALYSIS TODAY

Catalyst deactivation in the cracking of hexadecane and commercial FCC feed as studied by microactivity test–multiple cold trap (MAT–MCT) technique

P.M. Michalakos[a,*], R.C. Robinson[b], Y. Tang[a]

[a]*Chevron Petroleum Technology Co., La Habra, CA 90633, USA*
[b]*Chevron Research and Technology Co., Richmond, CA 94802, USA*

Abstract

The activity, selectivity, and coke formation of a fluid catalytic cracking catalyst were investigated by cracking hexadecane (C_{16}) and a commercial feed (FCC) over Grace–Davison Super D Magnum catalyst. A microactivity test (MAT) unit was used in combination with a multiple cold-trapping (MCT) apparatus to generate time-dependent data. The reaction temperature was 930°F and the cycle time was 3 min, during which the catalyst cracking activity decreased exponentially for both feeds. The final value of grams carbon/grams catalyst decreased in the order FCC/0.886>FCC/0.443>C_{16}. Interestingly, roughly 50% of the carbon formed was deposited within the first 20 s, and after 50 s the coking rates decreased by an order of magnitude. The catalyst activity versus carbon-on-catalyst curve shows three types of behavior. Initially, the catalyst is at its highest activity for both cracking and coking reactions. In the middle region, C_{16} cracking deactivates quicker because the strong active sites required for cracking a paraffin of low carbon number have been fouled. In contrast, the commercial FCC feed is reactive enough to be converted over sites with a wider range of acid strengths. Finally, the cracking and coking rates reach their lowest value, but are above thermal rates. For the commercial FCC feed, the gasoline/C_1–C_4 gas ratio was found to increase until the coke rate became constant. No significant changes in selectivity during the reaction cycle were observed for C_{16} cracking. From these data, it is proposed that C_{16} coke formation occurs in series with the cracking reaction, while the commercial feed makes coke in reactions occurring parallel to the cracking reaction.

Keywords: Fluid catalytic cracking (FCC); Microactivity test (MAT); Coke; Deactivation

1. Introduction

Fluid-catalytic cracking of vacuum gas oils could be processed for greater profitability if reliable kinetic-based models were available for refinery planning and on-line control [1–3]. Currently available semi-empirical models are dependent on reactor design and perform poorly when applied to conditions outside the range in which the parameters were derived. An important issue in developing new models is obtaining a kinetic expression for catalyst deactivation, a, which is applied to the intrinsic reaction rate, R_0, so that the reaction rate at some time-on-stream or coke level, R_i, can be determined:

$$R_i = aR_0. \quad (1)$$

*Corresponding author. Present address: Allied Signal, 50 E. Algonquin Rd., des Plaines, IL 60017, USA.

0920-5861/98/$ – see front matter
PII: S0920-5861(98)00347-2

The activity has often been expressed as a function of time-on-stream, but in mechanistic terms the activity is dependent on time only implicitly [4]. There is no agreement in the literature as to the exact mechanism by which an FCC catalyst loses its activity, but much work has been compiled in correlating deactivation with an increase in the amount of carbon-on-catalyst [5,6].

A commonly employed method of determining catalyst performance in the laboratory is the microactivity test (MAT) which is based on a fixed-bed reactor operated in a semi-batch mode (ASTM D3907). A charge of catalyst, which may be diluted with alumina to a fixed bed volume, is loaded, oil is fed for prescribed amount of time, and the product is collected for analysis. During a conventional MAT cycle the catalyst deactivates but this behavior cannot be studied because only one average conversion and product distribution may be calculated. Previous attempts to derive instantaneous measurements of conversion or coke versus time have required a pulse mode of introducing feed to the bed [7–9], but stripping and reactivation of the bed occurs between pulses; or using pre-coked samples [10], which requires repeating the reaction at different times and is therefore time consuming and typically accomplished for long cycle times.

In the present work, the activity function was determined as a function of the carbon-on-catalyst. A MAT unit was coupled to the multiple cold-trap apparatus (MCT), which can obtain up to 10 product samples from a process stream and hold them until ready for analysis by gas chromatography (GC). This represents the first construction of the transient reaction behavior for a MAT run. Added benefits of the MAT–MCT technique are that the data may be combined and compared with the MAT database, and that the MAT reaction may be better understood. This paper presents the results of the study of cracking of hexadecane (C_{16}) and a commercial FCC feed over Grace–Davison's Super D Magnum catalyst. The conversion, C_1–C_4 gas/gasoline ratio, and carbon-on-catalyst were measured as a function of time-on-stream. The experimental activity, a, was calculated according to Eq. (1). The activity and carbon-on-catalyst were mathematically modeled. These expressions were combined to eliminate time and obtain the desired correlation between the activity and the wt% carbon-on-catalyst. A comparison of these curves for C_{16} and the commercial feed gave

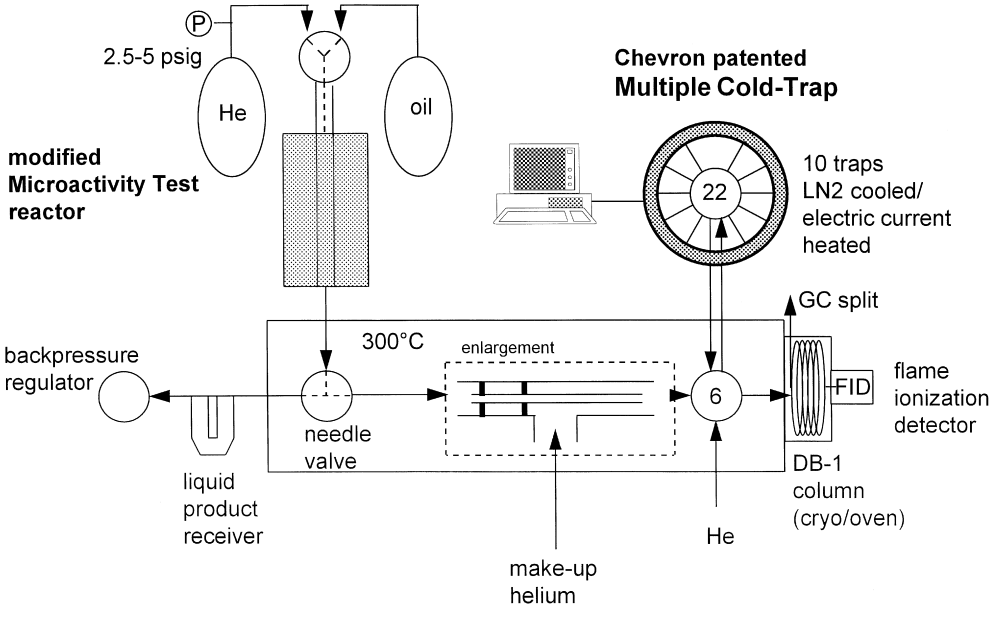

Fig. 1. Schematic of Chevron's patented multiple cold-trap (MCT) coupled with a microactivity test (MAT) reactor.

information that allowed a deactivation mechanism to be proposed.

2. Experimental

The experimental apparatus is shown in Fig. 1 and consisted of a microactivity test (MAT) unit attached to the Multiple Cold Trap (MCT), which is connected to a gas chromatograph (GC) equipped with a flame ionization detector (FID). The MAT reactor was operated at 930°F although a significant endotherm occurred during reaction. The endotherm was minimized by placing a heating rod inside the reactor before the bed. The feed at 150°F was pumped at 0.51 ml/min with 10 ml/min helium as carrier gas and

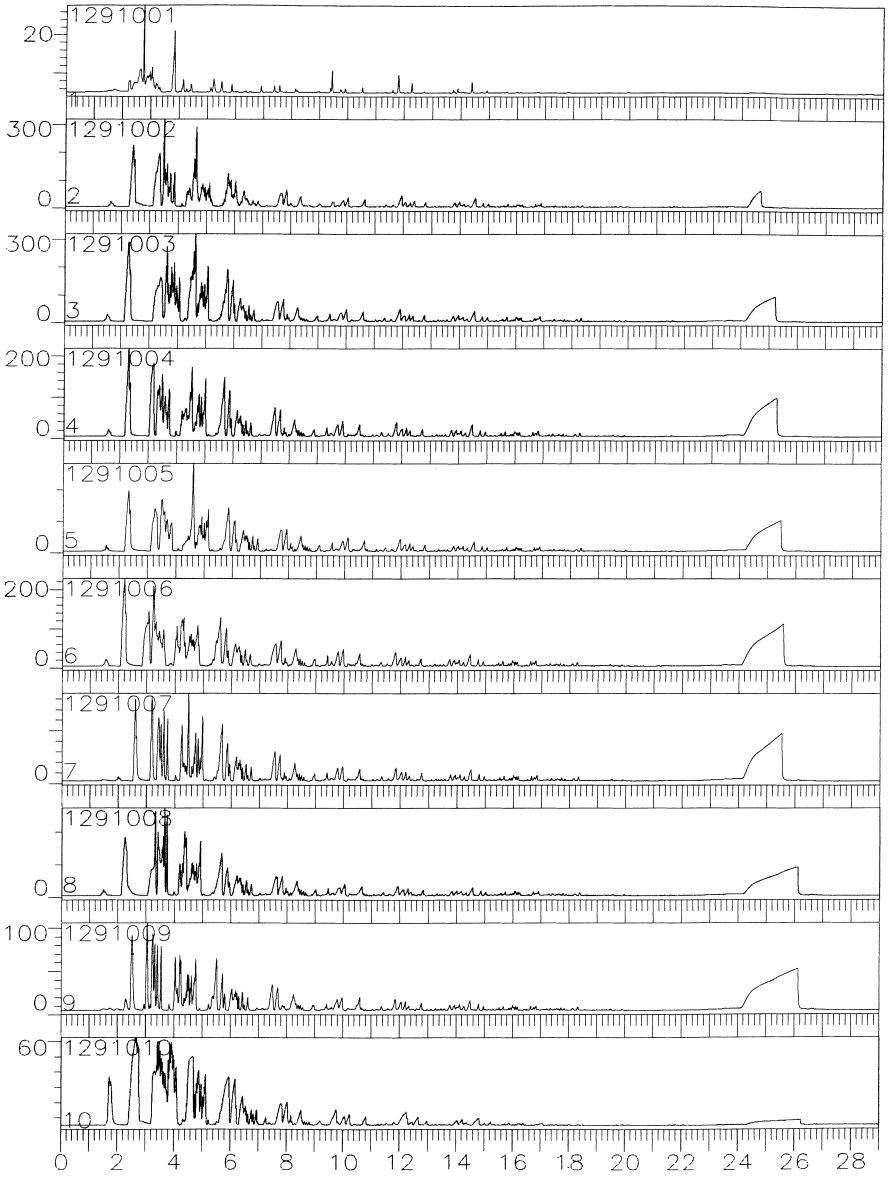

Fig. 2. GC–FID traces of the 10 traps.

vaporized as it passed through a metal preheat tube at 930°F in the quartz reactor. The reaction feed cycle lasted 3 min and was followed by 15 min of He to purge the catalyst. The feeds used were hydrotreated hexadecane, and a commercial FCC feed. The density of hexadecane was corrected for the feed pump temperature of 150°F to 0.741 g/ml using the HBT technique [11]. The commercial feed has an average molecular weight of 325 (internal measurement) and a density of 0.889 g/ml at 25°C, which was corrected to 0.853 g/ml at 150°F (internal measurement). The resulting vapor passed through a bed of either 0.443 g catalyst mixed with 2.786 g calcined alumina, or 0.886 g catalyst mixed with 2.435 g alumina. The calculated weight of catalyst to flow rate ratio (*W*/*F*) is listed in Table 1. The catalyst used for all tests was Super D Magnum (Grace–Davison), which consists of zeolite Y (a faujusitic structure) exchanged with 4.4% rare earth elements, combined with a silica–alumina matrix, and deactivated by steaming for 4 h at 1500°F so that the activity resembles that of an equilibrium catalyst. Alumina was prepared by calcination at 1100°C to minimize its surface area and thus its cracking activity. The reactor volume following the bed was minimized by packing with quartz chips.

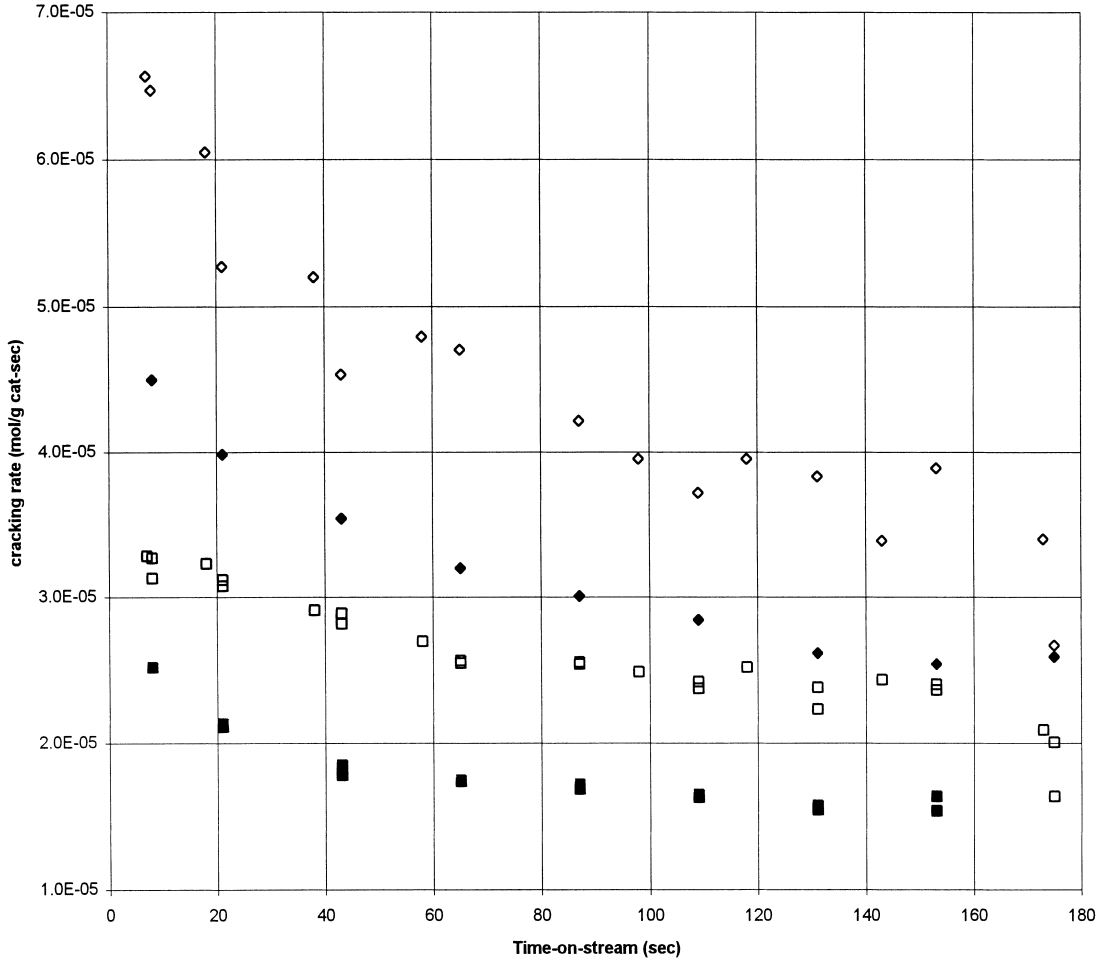

Fig. 3. Instantaneous rate of reaction. Hexadecane (C_{16}), open symbols. Commercial FCC feed, filled symbols. Squares, 0.886 g catalyst. Diamonds, 0.443 g catalyst.

Table 1
Parameters for fitting of cracking reaction data

	Hexadecane	Commercial FCC
Molecular weight *W/F* (g cat/g feed s)	226	325
0.886 g cat	142.2	117.25
0.443 g cat	71.10	58.63
Activity *A*	0.005139	0.221
k	0.000149	0.000312
t^*	8	8
n	1	0.224
$A^*(W/F)\hat{}n$	0.7308	0.64525
0.886 g cat	0.3654	0.550
0.443 g cat		
Carbon deposition		
a_1	0.01528	0.007494
k_1	0.005636	6.01e-05
a_2	0.00301	0.010671
k_2	0.6917	0.000497
m	0	1.0693

As the MAT unit is about 1000*x* oversized for the analytical apparatus, the following method of sampling the MAT effluent was devised. The effluent was split by a micro-control valve (SGE) into two flows, the majority to vent and a small flow to the MCT. The vented flow passed through a syncrude collection vessel at room temperature and finally through a back-pressure regulator (Porter Instruments) before venting to atmosphere. The flow of about 4.0 ml/min is sent to the MCT via a 0.25 μm capillary that passes through a 1/8 in tee fitting that supplies 10 ml/min of helium at 1.5 psig (Fig. 1). The micro-control valve and back-pressure regulator are adjusted so that the reactor pressure is initially 2.5 psig when the helium carrier gas through the bed is 10 ml/min. During the reaction when 0.51 ml/min of feed oil is vaporized and cracked, the pressure rises to 3.5–4.0 psig.

Descriptions of MCT and its applications have appeared in the literature [12,13]. Briefly, the MCT consists of a Valco 22-port 10-position valve that accepts sample from a heated transfer line and distributes it consecutively to ten traps. Each trap consists of a thin-walled U-shaped stainless steel tubing packed with 250 mm silica beads (Supelco), and is immersed in a liquid nitrogen filled Dewar during the trapping sequence and heated via electric current through the tubing during detrapping. The detrap conditions varied with feedstock. For C_{16}, each trap was heated to 300°C for 3 min and flushed to the GC with 70 ml/min He. This achieved a split ratio of 66:3=vent:column needed to limit the overloading of the C_{16} peak. For the commercial feed, each trap was heated to 330°C for 5 min and flushed with 15 ml/min so that the split ratio is 11:3. The sample is separated by a 0.25 mm i.d.×50 m capillary column with 100% polymethylsiloxane film of 0.25 μm thickness (Quadrex) and analyzed by a FID (Varian 3300). The detector response was linear over the sample areas encountered.

In a separate set of experiments where the reaction products were not analyzed, the feed time was varied and the amount of carbonaceous deposits remaining on a catalyst after 15 min stripping in flowing He at the reaction temperature were measured by a LECO machine. The deposits themselves will be referred to as ''coke''. When quantitatively referring to the deposits or the rate of deposition, the term ''carbon'' will be used because the LECO method does not measure the hydrogen present in the coke.

From the GC chromatogram, the conversion, activity, and selectivity was calculated. The fractional conversion, *x*, was defined as (sum of product areas)/(total chromatogram area). For C_{16}, the products comprise all peaks except C_{16}. For the commercial feed, the division between product and feed could be made where dodecane (b.p. 215°C) elutes. The fractional conversion could be expressed as a reaction rate by dividing by *W/F* (catalyst weight/molar feed rate), listed in Table 1. The activity at a given time, *a*, was defined as in Eq. (1) and calculated using the conversion from the first trap as the initial rate. The selectivity to gas is the area of C_1–C_4 products divided by sum of product areas, while the selectivity to gasoline was defined as the area from C_5 to C_{12} paraffins divided by the total area of products.

3. Results

A typical chromatographic profile for the trap series is shown in Fig. 2. For the first trap in each reaction, the amount of sample collected was 10% of that of subsequent traps, indicating that product from the

reactor reaches the MCT only about 20–22 s after the feed is started. This is consistent with the transfer time calculated from the internal volume of the flow path and the flow rate. The initial conversions are 95–99% except for the case of the commercial feed over 0.443 g catalyst. In general, the conversion for all cases decreased monotonically with time-on-stream. The average conversions (defined as the arithmetic average of all traps) were as follows: 73% and 65% for the commercial feed over 0.886 and 0.443 g catalyst, respectively; and 78% and 71% for C_{16} over the same catalyst amounts. This matches well with data collected on an unmodified MAT [14]. The conversions obtained over alumina only were 22% and 6% with the commercial feed and C_{16}, respectively.

The reaction rates were plotted as a function of a time-on-stream variable, *T*, which is defined below (Fig. 3). In this and subsequent graphs the reactions may be referred to by the feed, C_{16} or FCC (commercial feed) and by catalyst loading, 0.886 (high loading) or 0.443 (low loading). For each feed, the decrease in reaction rate over the reaction cycle time is proportionally less with the higher catalyst loading. This is shown clearly in the plot of activity versus time (Fig. 4). The activity was modeled by the following equation:

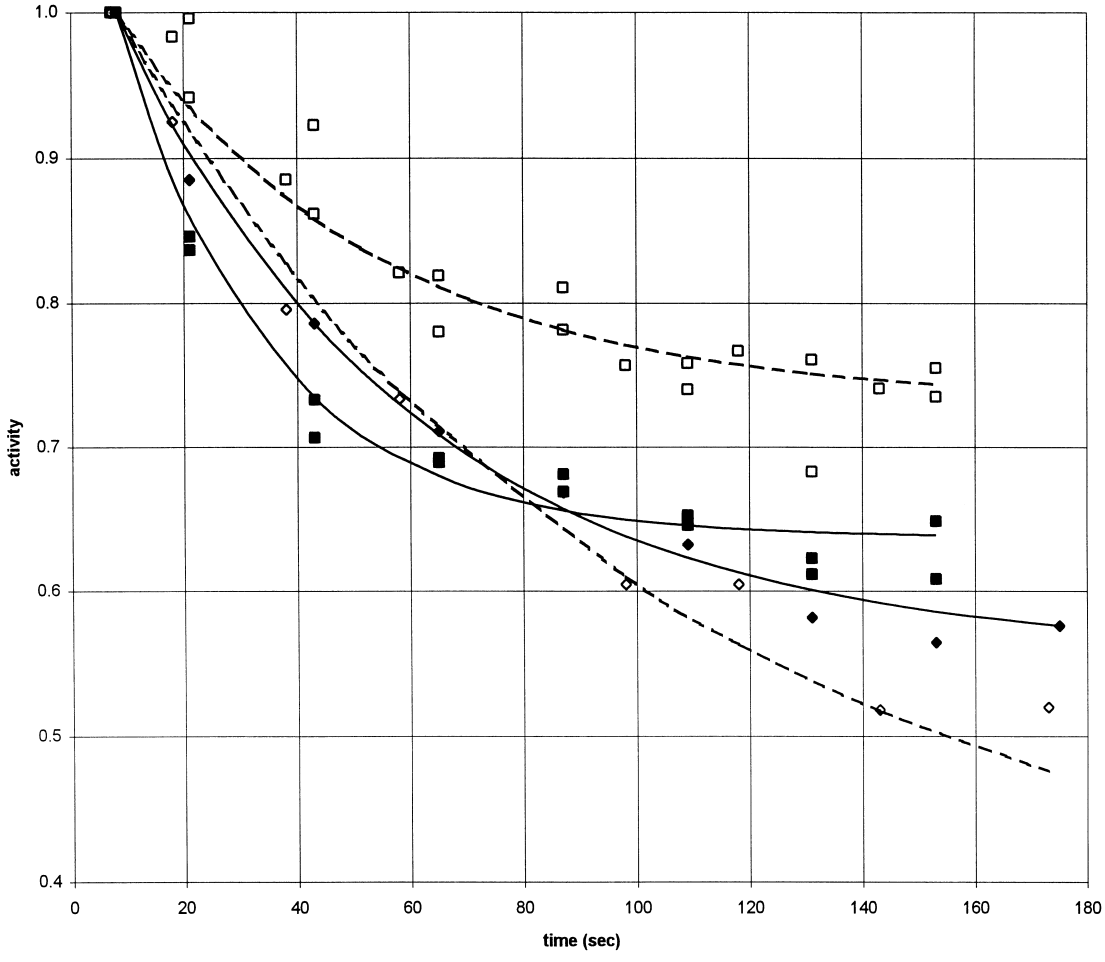

Fig. 4. Comparison of activity: Hexadecane (C_{16}), open symbols. Commercial FCC feed, filled symbols. Squares, 0.886 g catalyst. Diamonds, 0.443 g catalyst. Curves according to Eq. (2).

Table 2
Trap schedule (feed begins at t=0 s)

Trap	Time trap closes (s)	Plot time (s)
1	22	8
2	44	19
3	66	41
4	88	63
5	110	85
6	132	107
7	154	129
8	176	151
9	198	173
10	1100	

$$a = (1 - A(W/F)^n)\exp(-k(W/F)(T - t^*)) + A(W/F)^n. \quad (2)$$

The deactivation rate constant, k, was 0.000312 and 0.000149 g feed/g cat s^2 for the commercial feed and C_{16}, respectively. The value of A is listed in Table 1 and is related to the catalyst activity extrapolated to infinite time. The exponent n was unity for hexadecane but a fractional value for the commercial feed. The time T was the midpoint of the opening and closing times of each trap adjusted for the time required for product to reach the trap from the catalyst bed, approximately 14 s (Table 2). This time was determined by subtracting from the transfer time the delay in feed reaching the catalyst bed from the feed valve, t^*, about 6–8 s based on the following observations: feed exits the feed tube leading to the reactor 6–8 s after starting the feed pump; the bed temperature decreases after about 10 s, which reflects the point that the colder feed reaches the bed and the endotherm associated with reaction (a typical midbed temperature–time profile is presented in Table 3). The parameter t^* allows the equation to satisfy the boundary condition a=1 at t=0; that is, $(T-t^*)$ is the true reaction time-on-stream, t.

The amount of carbon deposited per gram of catalyst during the reaction is presented in Fig. 5. A set of reactions using only alumina was used to correct for carbon deposited on alumina. In general, the curve has two regions, the first lasting from 0 to 50 s for FCC and 0 to 20 s for C_{16}. The total carbon amount decreased in the order FCC/0.886>FCC/0.443>C_{16}, with the differences between cases attributed to the rate and duration of the first region. For all cases, at least 50% of the total carbon was deposited within the first 20 s; this rate was 4.15×10^{-5} mol carbon/g cat s for FCC/0.886 and 2.68×10^{-5} mol carbon/g cat s for FCC/0.443 and C_{16}. The average rates between 80 and 180 s were an order of magnitude less than the initial rates: 2.6×10^{-6} and 2.68×10^{-5} mol carbon/g cat s for FCC and C_{16}, respectively. The data were fitted with a linear combination of two terms to describe each region:

$$C = a'(1 - \exp(-(W/F)^m k' t) + a''(1 - \exp(-(W/F)^m k'' t) \quad (3)$$

Carbon deposition was independent of the space velocity for C_{16} (m=0) but not for the commercial feed (m=1). The parameters are presented in Table 1. The time t is the true reaction time and does not require correction; it is equivalent to the quantity $(T-t^*)$ in Eq. (2). By substitution of $(T-t^*)$ for t in Eq. (3), a relationship between carbon-on-catalyst and catalyst activity is obtained:

$$C = a'(1 - \exp(-(W/F)^m k'(1/((W/F)k)) \times \ln((x - A(W/F)^n)(1 - A(W/F)^n))) + a''(1 - \exp(-(W/F)^m k''(1/((W/F)k)) \times \ln((x - A(W/F)^n)(1 - A(W/F)^n))). \quad (4)$$

Table 3
Catalyst midbed temperature during cracking (C_{16} over 0.886 g catalyst)

t (min)	T (°C)
0.00	931
0.30	923
0.40	905
0.60	884
0.80	881
1.00	891
1.20	884
1.40	892
1.60	902
1.80	907
2.00	918
2.20	925
2.40	916
2.60	917
2.80	926
3.00	928

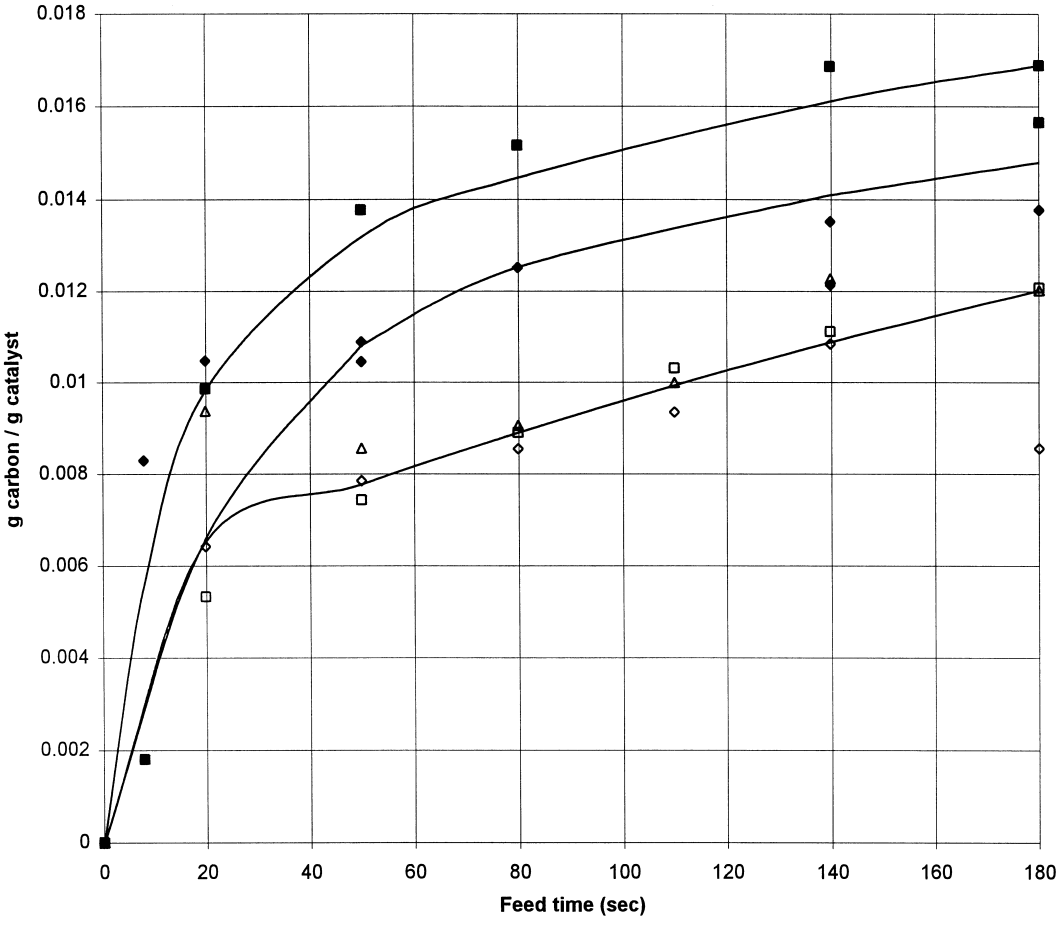

Fig. 5. Carbon deposition comparison of activity: Hexadecane (C_{16}), open symbols. Commercial FCC feed, filled symbols. Squares, 0.886 g catalyst. Diamonds, 0.443 g catalyst. Triangles, 0.22 g catalyst. Curves according to Eq. (3).

Eq. (4) is plotted in Fig. 6. This plot shows three types of behavior: initially, the catalyst is at its highest activity for both cracking and coking reactions; in the middle region, C_{16} cracking deactivates more quickly; finally, the cracking and coking rates reach their lowest value, but are above thermal rates.

Fig. 7 examines the selectivity to two lumps, gasoline (C_5–C_{12}) and gas (C_1–C_4). In the cracking of the commercial feed, the gasoline/C_1–C_4 gas ratio was found to increase until about 50 s, which is when the carbon deposition rate became constant. For C_{16}, the selectivity to these lumps was not a strong function of time-on-stream.

4. Discussion

A comparison between the data reveals the following interesting results that will be discussed:

1. The dependence of both cracking activity and coking on (*W*/*F*) is different between feeds.
2. Initially, the fractional conversions for each feed are similar with different catalyst loadings, but in the second half of the reaction cycle there is more deactivation with the lower catalyst loading.
3. The amount of carbon deposited on the catalyst is greater with the commercial feed than C_{16}.

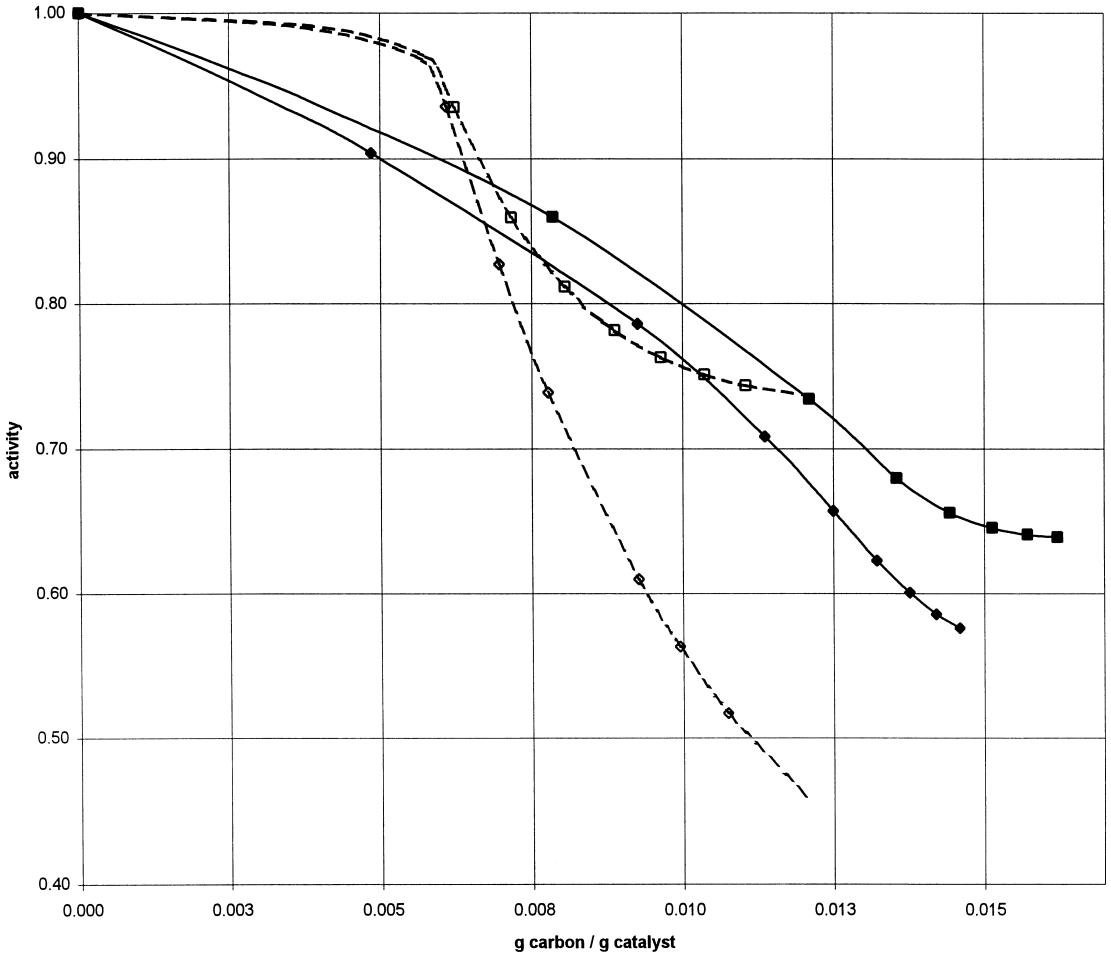

Fig. 6. Comparison of deactivation. Hexadecane (C_{16}), open symbols. Commercial FCC feed, filled symbols. Squares, 0.886 g catalyst. Diamonds, 0.443 g catalyst. Curves according to Eq. (4).

4. The activity for C_{16} decreases sharply at 0.007 g carbon/g catalyst, while that for the commercial feed decreases gradually.
5. There is an initial increase in the selectivity of the commercial feed to gasoline, but little change with C_{16}.

The reaction rates per gram catalyst plotted in Fig. 3 are greater for reactions using lower catalyst loadings, which is characteristic of an integral reactor where the feed concentration decreases over the catalyst bed. The most reactive molecules crack first, so the reactivity of the feed and thus the conversion will decrease with increasing weight of catalyst seen by the feed. For both the commercial feed and C_{16}, the conversion from increased amounts of catalyst is small enough that the rate is artificially lowered when averaged over the weight of catalyst in the bed, and the rate per gram of catalyst is lower for higher catalyst loadings. However, as the catalyst at the beginning of the bed deactivates, there is more feed unconverted, which passes to catalyst that is more active than at the beginning of the bed and is converted (high loading case) while it passes out of the bed (low loading case). This explains the greater deactivation of the low loading beds.

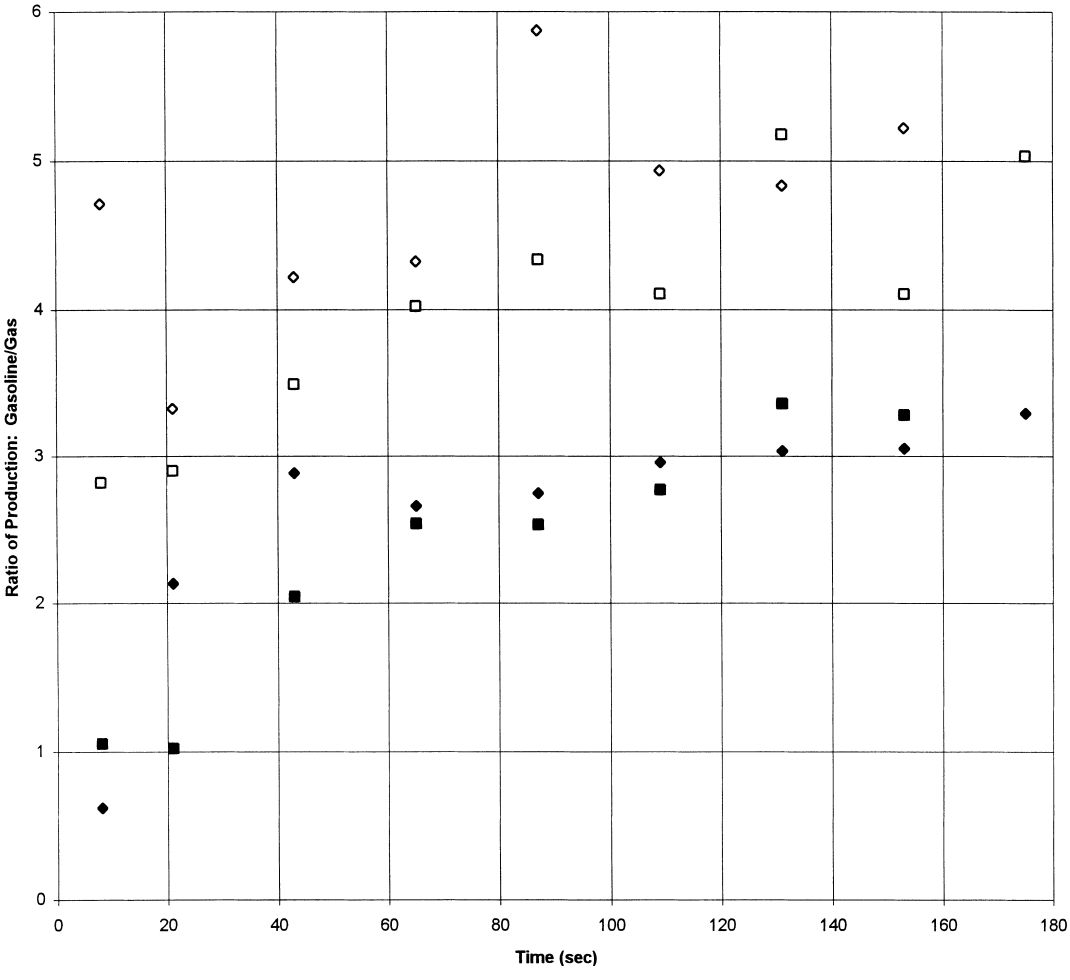

Fig. 7. Comparison of gasoline selectivity. Hexadecane (C_{16}), open symbols. Commercial FCC feed, filled symbols. Squares, 0.886 g catalyst. Diamonds, 0.443 g catalyst.

In addition to changing feed composition and catalyst deactivation, the rate of reaction will be affected by the "multiplicity of molecular types present" in the feed [15]. The range of reaction velocities of the different molecules causes a pseudo-first order reaction to appear to have a larger apparent reaction order. Some workers have taken this nonlinear dependence into account by using a psuedo-second-order model. In the present work these effects have been taken into account by letting the exponent n in Eq. (2) take a fractional value, while because C_{16} is a single component feed, n=1. This allows the general form of the equations to be the same for both feeds.

The behavior of the first region of the carbon deposition curve may be explained by the differences in the feed composition. Commercial feeds are vacuum gas oils containing paraffins with carbon numbers greater than 16, naphthenes, aromatics, sulfur and typically 1000–2000 ppm nitrogen. In general, the cracking rate increases with increasing molecular weight [16], and coke formation increases with increasing aromatic [7,17,18] and nitrogen-heterocyclic compounds [19,20]. Many mechanisms for coke formation have been proposed. One path begins with the cracking of paraffins [21,22] or alkyl aromatics [21,23]. The olefins that are produced dehydrogenate

to form dienes and subsequently trienes, then cyclize to aromatic compounds [22,23]. A second pathway is directly from nitrogen-containing compounds and multi-ring aromatics. Once the initial aromatic structure is formed, there is further ring growth accompanied by release of hydrogen and light gas [6,10,24].

Coke formation is a self-deactivating reaction in that after the initial period of high coking activity the increase in coke formation decreases by an order of magnitude. The first region could be interpreted as the initial formation of coke molecules with 2–3 rings. According to the general mechanism discussed above, this rate would be directly related to the feed's ability to generate olefins from paraffins or alkyl chains. The greater reactivity of gas oils plus the nitrogen content result in higher coke levels than from C_{16}. The behavior observed in the second region is consistent with increasing the number of rings of coke molecules that were formed in the first region, which is slower than generation of new coke molecules [25]. The fact that the coke versus time curve for the commercial feed increases with *W/F* ratio implies that there is a nonlinear dependence of coke activity on weight of catalyst. This reflects the nonlinearities of the greater number of coke-forming reactions than for C_{16}.

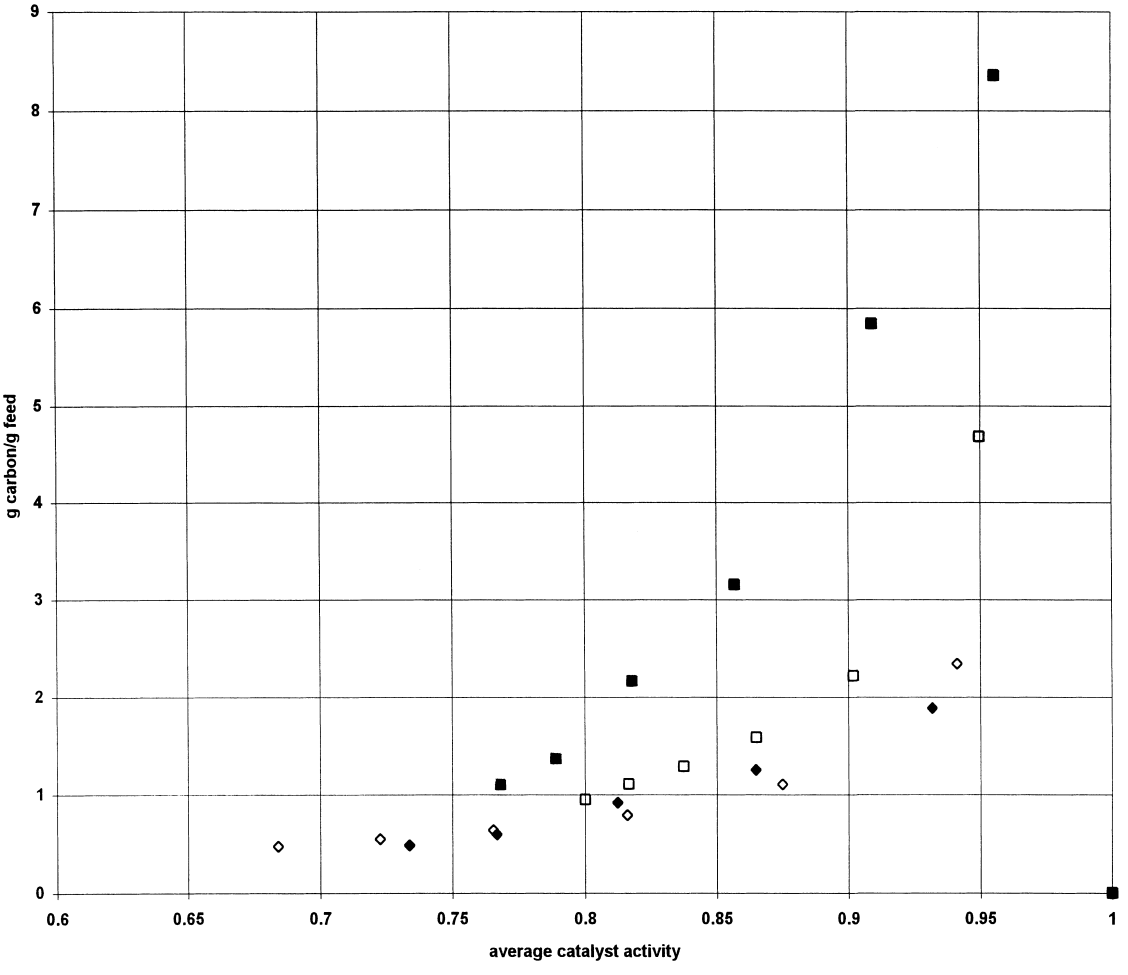

Fig. 8. Dependence of coke yield and catalyst activity on cat/oil. Hexadecane (C_{16}), open symbols. Commercial FCC feed, filled symbols. Squares, 0.886 g catalyst. Diamonds, 0.443 g catalyst.

The cracking deactivation rate constant in Eq. (2) for the commercial feed is twice that for C_{16}, and the initial carbon deposition rate is also greater for the commercial feed, indicating a strong correlation between activity and coke. In Fig. 6, this relationship may be explored by comparing activities at constant carbon, or by comparing carbon at constant activity. Because the activity at a given carbon level is different for each combination of catalyst charge and feed, there is no universal activity versus coke curve. One explanation is that the reactivities of the feeds are different, that is, the commercial feed reacts on sites having a wider range of acid strengths, so the total number of sites available for reaction is larger for a gas oil than C_{16}. A compound of relatively low reactivity such as C_{16} cracks more on the strongest acid sites only [26]. Because these sites are fouled quickest [6,26–28], the activity decreases with a smaller amount of coke. This explains the sharp drop in catalyst activity at 0.007 g carbon/g catalyst (Fig. 6) compared to curve for the commercial feed. The compounds in gas oils may react over sites with a wider range of acid strengths, and catalyst deactivation is gradual. However, because the commercial feed has greater coke formation and greater deactivation, the average activity is slightly lower than for C_{16}.

An alternate method of examining Fig. 6 is to consider the coke levels at a given activity. After

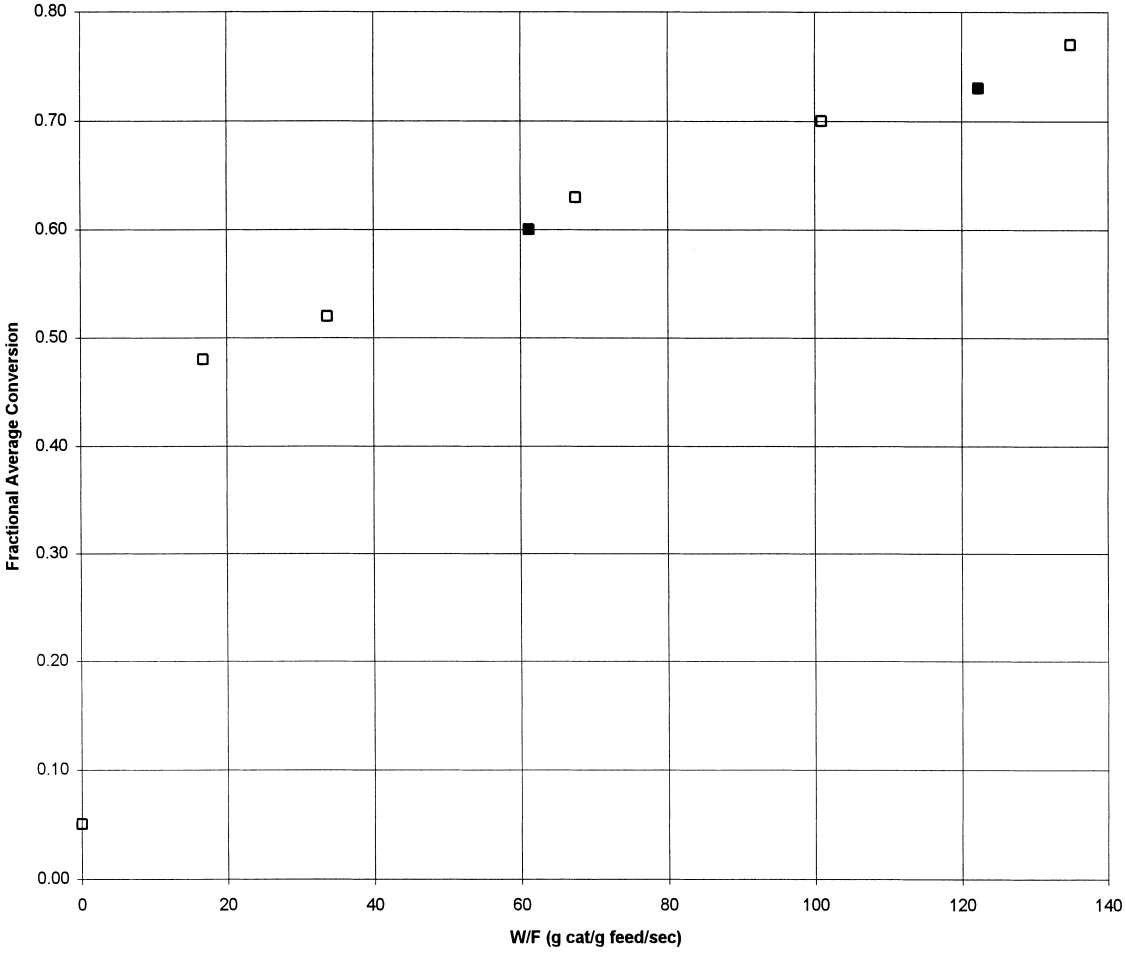

Fig. 9. Average conversion as a function of *W/F*. Hexadecane (C_{16}), open symbols. Commercial FCC feed, filled symbols.

0.9 activity, the carbon levels are higher for the commercial feed. This implies that the selectivity to coke is higher. Indeed, at a given conversion the coke yields are higher for the commercial feed (Fig. 8).

The assumption of the effect of coke on activity is that a given amount of coke in one reaction is physically similar as the same amount derived from a different feed or reaction. The coke has not been characterized with respect to C/H ratio (which is typically 1 [4,22]) or number of rings; however, the carbon measured in these experiments is after a 15 min stripping time and should be free of ''soft coke'', e.g. carbonaceous materials that may play a role on the catalyst surface during reaction or hydrocarbons that fill the catalyst pores.

The changing selectivity for cracking of the commercial feed may be related to either the decrease in rate of cracking or of coke formation. Overcracking (formation of C_1–C_4 gas) may occur when the most reactive fractions of the feed crack over the strongest active sites. As the sites are fouled, the gasoline/C_1–C_4 ratio will increase to a constant value. This may explain why the selectivity becomes constant at the same time the rate of coke formation does, about 50 s (Figs. 4 and 5). A small amount of C_1–C_4 gas produced in the initial period may be a by-product of coke formation parallel to the cracking reaction [6,7,10,24]; therefore, the rates of formation of coke and gas decrease to a constant value.

It is noted that it is not necessary to use pore plugging to explain the deactivation phenomena observed in this study. This is justified by considering the following points. There is not a strong mass transfer limitation on conversion, as shown in Fig. 9. The linear dependence of conversion on the weight of catalyst only changes at 0 g catalyst. The zeolite dimensions are large compared to the reactants, and the amount of coke is low enough so that there is low possibility of pore-plugging by coke from small molecules. For example, the critical molecular dimension of *n*-paraffins is 4 Å, of benzene, 2-methyl olefins, and iso-paraffins is 5-5.7 Å, and of naphthalene, 7.25 Å. The channel dimension of the zeolite is 7.25 Å and the cavity is 11.7 Å, and the active matrix of the catalyst cracks the larger molecules before they enter the zeolite. The carbon-on-catalyst levels are low compared to literature reports where pore plugging has been considered important (1–1.5% versus 3–5 wt%).

For the data generated by the MAT–MCT to be relevant to commercial application, the fundamental concepts must be extracted and reduced to a mechanistic scheme with rate expressions. At this point, the

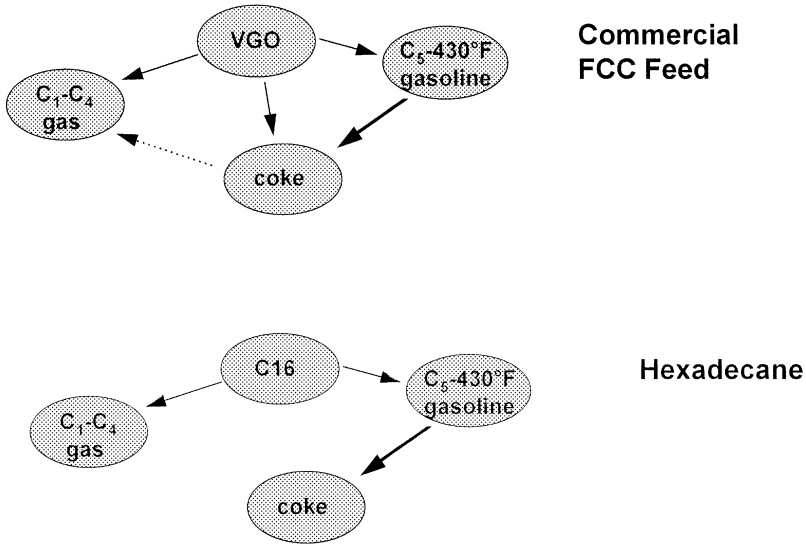

Fig. 10. Lumped model for cracking.

available data allow a simple scheme to be proposed. In the case of C_{16}, coke is formed by reactions subsequent to the cracking reaction, typically dehydrocyclization of olefins. From the commercial feed there are pathways occurring parallel to the cracking reactions, such as formation from multi-ring aromatics and naphthenes and nitrogen-containing compounds that do not undergo cracking (Fig. 10).

5. Conclusion

The deactivation of Super D Magnum, a commercial cracking catalyst, in the cracking of a commercial FCC feed and hexadecane could be explained by the deposition of carbon on the catalyst to form coke. With both feeds, the cracking and carbon formation rates are highest at the beginning of the reaction when there is no or little carbon on the catalyst. The activity and carbon versus time curves were fitted in order to mathematically express the dependence of activity on carbon. As carbon is deposited on the catalyst and coke is formed, both the cracking and carbon deposition rates decrease. The commercial FCC feed contains molecules with higher molecular weights which increase the rate of formation of olefins, and it also contains aromatics, naphthenes, and sulfur and nitrogen heterocyclic compounds that are strong coke precursors. Therefore, the initial carbon deposition rate and the final carbon level for the commercial feed is greater than with C_{16}. Although C_{16} produces less coke it requires the strongest active sites for cracking, which are poisoned first. The net effect is that the average conversion over a 3 min cycle is only slightly greater for cracking of C_{16} than the commercial feed. The information generated from this study will be used with detailed data on the product distribution in order to propose a mechanistic scheme for a kinetic model that is applicable to an FCC unit.

Acknowledgements

The authors thank Henri Lese and Anil Patel for helpful discussions, and Larry Babb for LECO carbon analyses.

References

[1] J.S. Magee, W.S. Letzsch, in: Fluid Catalytic Cracking III, ACS, Washington, DC, 1994, p. 349.
[2] D.W. Kraemer, U. Sedran, H.I. de Lasa, Chem. Eng. Sci. 45(8) (1990) 2447.
[3] P. Turlier, M. Forissier, P. Rivault, J.R. Bernard, in: Fluid Catalytic Cracking III, ACS, Washington, DC, 1994, p. 98.
[4] J.B. Butt, E.E. Peterson, Activation, Deactivation, and Poisoning of Catalysts, Academic Press, San Diego, 1988.
[5] B.W. Wojciechowski, Cat. Rev.-Sci. Eng. 9(1) (1974) 79.
[6] B.W. Wojciechowski, A. Corma, Catalytic Cracking: Catalysts, Chemistry, and Kinetics, vol. 19, Marcel Dekker, New York, p. 128.
[7] J. Corelia, E. Frances, in: C.H. Bartholomew, J.B. Butt (Eds.), Catalyst Deactivation 1991, Elsevier, Amsterdam, 1991, p. 375.
[8] J.W. Dean, D.B. Dadyburjor, Ind. Eng. Chem. Res. 28 (1989) 271.
[9] F. Hershkowitz, P.D. Madiara, Ind. Eng. Chem. Res. 32 (1993) 2969.
[10] M. Forissier, J.R. Bernard, in: C.H. Bartholomew, J.B. Butt (Eds.), Catalyst Deactivation 1991, Elsevier, Amsterdam, 1991, p. 359.
[11] R.C. Reid, J.M. Prausnitz, B.E. Poling, Properties of Gases and Liquids, 4th ed., McGraw Hill, New York, 1988.
[12] Y. Tang, M. Tauffer, Org. Geochem. 22(3–5) 863.
[13] Y. Tang, M. Stauffer, J. Appl. Anal. Pyrolysis 28 (1994) 167.
[14] H. Lese, Chevron Research and Technology Corporation, unpublished results.
[15] V.W. Weekman Jr., Ind. Eng. Chem. Proc. Des. Dev. 7(1) (1968) 90.
[16] Y.V. Kissin, J. Catal. 126 (1990) 600.
[17] D.M. Nace, S.E. Voltz, V.W. Weekman Jr., Ind. Eng. Chem. Proc. Des. Dev. 10(4) (1971) 531.
[18] S.E. Voltz, D.M. Nace, V.W. Weekman Jr., Ind. Eng. Chem. Proc. Des. Dev. 10(4) (1971) 539.
[19] S.E. Voltz, D.M. Nace, S.M. Jacob, V.W. Weekman Jr., Ind. Eng. Chem. Proc. Des. Dev. 11(2) (1972) 261.
[20] J. Scherzer, in: Fluid Catalytic Cracking III, ACS, Washington, DC, 1994, p. 145.
[21] W.S. Letzsch, A.G. Ashton, in: J.S. Magee, M.M. Mitchell Jr. (Eds.), Fluid Catalytic Cracking: Science and Technology, Elsevier, Amsterdam, 1993, p. 441.
[22] C. Naccache, in: J. Oudar, H. Wise (Eds.), Deactivation and Poisoning of Catalysts, Marcel Dekker, New York, p. 185.
[23] J.W. Hightower, P.H. Emmett, J. ACS 87(5) (1965) 939.
[24] D.E. Walsh, L.D. Rollman, J. Catal. 49 (1977) 309.
[25] M. Guisnet, P. Magnoux, C. Canaff (CA-2-5), p. 701.
[26] G. Bourdillon, C. Gueguen, M. Guisnet, Appl. Catal. 61 (1990) 123.
[27] P. Magnoux, P. Cartraud, S. Mignard, M. Guisnet, J. Catal. 106 (1987) 242.
[28] A. Humphries, D.H. Harris, P. O'Connor, in: J.S. Magee, M.M. Mitchell Jr. (Eds.), Fluid Catalytic Cracking: Science and Technology, Elsevier, Amsterdam, 1993, p. 41.